Research of the Failure Mechanism and Preventive Strengthening of Prefabricated Small Box Girder under Car Explosion

Wenliang Hu , Fenghui Dong * , Zinan Yu *

Posted Date: 19 March 2024

doi: 10.20944/preprints202403.1125.v1

Keywords: Failure mechanism; Preventive strengthening; Prefabricated small box girder; Car explosion

Article

Research of the Failure Mechanism and Preventive Strengthening of Prefabricated Small Box Girder under Car Explosion

Wenliang Hu [1], Fenghui Dong [2] and Zinan Yu [3,4,*]

[1] Northwestern Polytechnical University, Xi'an, Shaanxi 710064, China.
[2] Nanjing Forestry University, Nanjing 210037, China
[3] Chang'an University, Xi'an, Shaanxi 710064, China.
[4] Chinaroads Communications Science Technology Group Co. Ltd, 8th Floor Building C Oriental Kenzo Dongdhimen, Dongcheng District, Beijing 100027
* Correspondence: 2016021022@chd.edu.cn

Abstract: The purpose of this study is to investigate the failure mechanism and preventive strengthening methods of prefabricated full length small box girder (PSBG) under car explosion. After damage analysis during blast loads using the commercial software Autodyn, three strengthening methods are presented to improve the blast mitigation performance. The results show that the failure modes and bearing capacity are significantly different with various strengthening measures. Adhering U-shaped steel plate can effectively enhance the shear performance of PSBG under blast loads. Strengthening the bottom of the upper flange of box girder with steel plate can effectively mitigate the local bending failure, and enhance the overall flexural capacity during car explosion.

Keywords: failure mechanism; preventive strengthening; prefabricated small box girder; car explosion

1. Introduction

With increasing of terrorist attacks in recent years, many researchers have focused on the study of dynamic responses and failure behaviors of reinforced concrete (RC) and prestressed concrete (PC) structures subjected to intentional and unintentional blast loads [1]. As an excellent superstructure in accelerated bridge construction, prefabricated small box girder has been widely used in highway bridges and urban viaducts. However, due to the characteristic of thin-walled members and the degradation of concrete and steel during explosion, the failure mechanism and preventive strengthening methods have become an urgent problem to be solved.

Besides terrorist attacks, unintentional explosions induced by vehicles and fireworks usually lead to severe damage even collapse of the bridge. Wang and Liu et al. [2] investigated the structural response of a multi-T-shaped bridge due to the dynamic load explosion. Zhai et al. [3] investigated the performances of RC structures subjected to blast loading after fire exposure, a series of model tests on RC beams were carried out. Experimental and numerical results showed that more and more cracks emerged at the mid-span zone of the beam under blast loads as the fire duration increased, and the peak and residual displacement of the RC beam increased nearly linearly with the fire duration. Zhu and Li et al. [4] studied a steel-concrete composite bridge under car explosion, and the damage mechanism was put forward to improve the explosion-resistant design of structures. Hu et al. [5] studied the dynamic responses and failure modes of prestressed T beams under blast loads, finite element models for the concrete beams based on LS-DYNA were established using the fluid-solid coupling method to perform dynamic analysis of constructions under different TNT weights, detonation locations, and stress conditions.

Zhang and Gholipour et al. [6] evaluated the nonlinear dynamic behaviors and failure modes of simply-supported reinforced concrete beams subjected to the combination of impact and blast loads. After comparison with experimental results and numerical simulations, the damage mode of RC

 doi:10.20944/preprints202403.1125.v1

beams under blast loading was concluded to be: local response, global flexural failure, global shear failure and global flexural-shear failure. Compared with the damage characteristics shown in Figure 1, the failure mode of PSBG is determined by damage coefficient and damage distribution in this work.

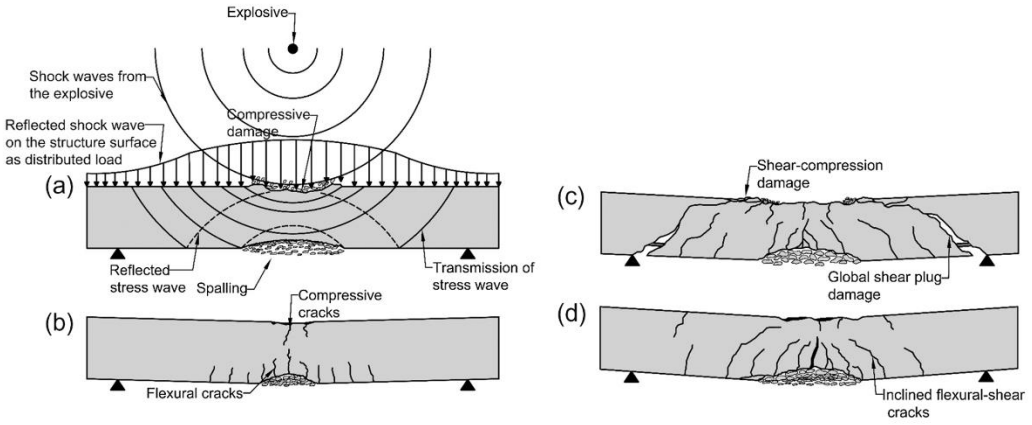

Figure 1. Theoretical response of RC beams subjected to air blast loading: (a) local response; (b) global flexural failure; (c) global shear failure; (d) global flexural-shear failure [6].

Shiravand and Parvanehro [7] studied the behavior of a typical concrete cantilever bridge under close-in deck explosion and provided the distribution of damage zone. Therefore, it was necessary to apply some energy absorbing or properly fused systems to reduce the close-in deck explosion effects. Lee and Choi et al. [8] suggested a procedure to assess structural blast-resistance performance based on a numerical analysis approach.

There are several strengthening measures available to improve the working performance of concrete beams in response to their decreased operational state [9–11]. However, there is a lack of relevant research on the failure mechanism and preventive strengthening of preventive small box beams under car explosion. In this article, the existing PSBG which widely used in highway bridges and urban viaducts are studied. The thickness of the bridge deck, reinforcement ratio and the strengthening steel plate meet the requirements of the existing design specifications [12,13]. According to existing cars, the fuel tank capacity and gasoline density are 70 L and 0.72kg/L respectively. Therefore, the internal energy of gasoline is similar to TNT.As a result, the 50kg TNT equivalent is proposed to present car explosion in the state of full oil-tank. Due to small lifting weight and convenient construction, simply supported beam becomes competitive in accelerated bridge construction (ABC). Under high pressure shock wave induced by explosive energy, more serious damage even bridge collapse is recognized when explosion happens in mid-span. To analyze the antiknock performance of multi-box girders bridge, the 50 kg TNT equivalent of the car explosion is placed above the top deck in the mid-span. The results of this study are of great significance for the failure mechanism and preventive strengthening of prefabricated box girder under car explosion.

2. Material Constitutive and Finite Element Modeling

2.1. Material Constitutive

Explosion induced energy usually release instantly and tremendously, resulting in high-strain rate [14] and high temperature field [7] of structures. The results of impact test showed concrete strength hardening under high-strain rate loading such as vehicle collision and blast loads [15]. Besides that, it was considered that the characteristic of concrete softening under high temperature could not be ignored in blast analysis. To accurately describe the distribution of stress and failure mode of structures under blast loads, the Riedel-Hiermaier-Thoma (RHT) model is adopted [16]. Material parameters are shown in Table 1.

 doi:10.20944/preprints202403.1125.v1

Table 1. Material parameters of concrete.

Compressive Strength (fc)(MPa)	Tensile Strength (ft/fc)	Shear Strength (fs/fc)	Elastic modulus (MPa)	Shear modulus (MPa)
32.4	0.1	0.18	32500	13000

The dynamic constitution of steel has become the main factor to control the accuracy of structural impact analysis. The results of experiment and numerical analysis verify the validity of Johnson-Cook (JC) model in simulating the strain rate sensitivity and the thermal softening of steel [17]. The flow stress is calculated by equation 1, while ε_p and ε_p^* stand for the effective plastic strain and normalized effective plastic strain rate respectively.

$$Y = (A + B\varepsilon_p^n)(1 + C\ln\varepsilon_p^*)(1 - T_H^m) \tag{1}$$

Where *A*, *B*, *C*, *n* and *m* represent initial yield stress, hardening constant, hardening exponent, strain rate constant and thermal softening exponent respectively [18] as shown in Table 2.

Table 2. Material parameters of JC equation state.

Material	Parameter *A* (MPa)	Parameter *B* (MPa)	Parameter *C*	Parameter *n*	Parameter *m*
Steel bar	330	405.9	0.26	0.014	1.03
Prestressed tendon	1860	2287.8	0.26	0.014	1.03
Steel plate	345	424.4	0.26	0.014	1.03

The ideal air is presented to simulate air pressure as shown in equation 2:

$$P = (\gamma - 1)\rho e \tag{2}$$

Where e represents a standard atmosphere pressure at the initiation of the explosion, γ is the adiabatic index of ideal air, and ρ is the material density, as shown in Table 3.

Table 3. Material parameters of air.

ρ (g·cm^{-3})	e (J·kg^{-1})	γ
0.00125	2.068×10^5	1.4

In order to obtain a precise analysis of the interaction between explosive pressure and energy, Jone-Wilkins-Lee (JWL) state equation is adopted here. The JWL equation is as follows:

$$P = A\left(1 - \frac{\omega}{R_1 V}\right)e^{-R_1 V} + B\left(1 - \frac{\omega}{R_2 V}\right)e^{-R_2 V} + \frac{\omega E_0}{V} \tag{3}$$

Where P stands for the pressure under blast loads, V is the volume ratio, E_0 is the internal energy, and *A*, *B*, R_1, R_2, and ω are material parameters, values of which are indicated in Table 4.

Table 4. Material parameters of JWL equation state.

Parameter R_1	Parameter R_2	Parameter *A* (MPa)	Parameter *B* (MPa)	Parameter ω	Density ρ (g·cm^{-3})	V	E_0 (J·kg^{-1})
4.15	0.90	3.378×10^5	3.747×10^3	0.35	1.63	1.00	7.0×10^6

3.2. Numerical Model

Due to the high insecurity of anti-explosion test [19–22], numerical analysis method becomes an effective way to analyze the damage of structure under blast loads [23–29]. This paper presents a 25

 doi:10.20944/preprints202403.1125.v1

m prefabricated small box girder with simply supported condition and the antiknock performance is studied. The height of the beam is 155 cm, including 140 cm for box girder and 15 cm for deck pavement. In order to accurately reflect the dynamic response and damage distribution under explosion, the arrangement of steel bars is consistent with the design drawings. The longitudinal steel bars adopt a diameter of 22 mm with a reinforcement ratio of 1.37%. To avoid shear failure under design loads, the diameter of stirrups is selected to be 12mm with a spacing of 10 cm around supporting point in 5 m. Except for large shear zone, the spacing of stirrups is determined to be 20 cm. Beam 161 is presented to simulate the reinforcements with rigid body rotation and finite strains during blast loads. To ensure the bonding property between reinforcements and concrete, sheared nodes are adopted. Besides that, transverse and longitudinal reinforcements are interconnected to stand for steel skeleton. An ideal non-slip connection is established between prestressed tendons and concrete. The initial prestress of prestressed tendon is 1395MPa with equivalent strain. Self-weight is considered with the gravitational acceleration of 9.8 m/s^2. Convergence studies conducted by Pan et al. [30] showed that a 10 cm mesh size was adequate to ensure a reliable pressure time-history and dynamic structural response compared with the experimental data. Further, the air mesh size and explosive mesh size were suggested to be 10 cm in this work. In order to balance the calculation accuracy and the arrangements of steel bars, the element size of 10 cm is adopted in this study as shown in Figure 2.

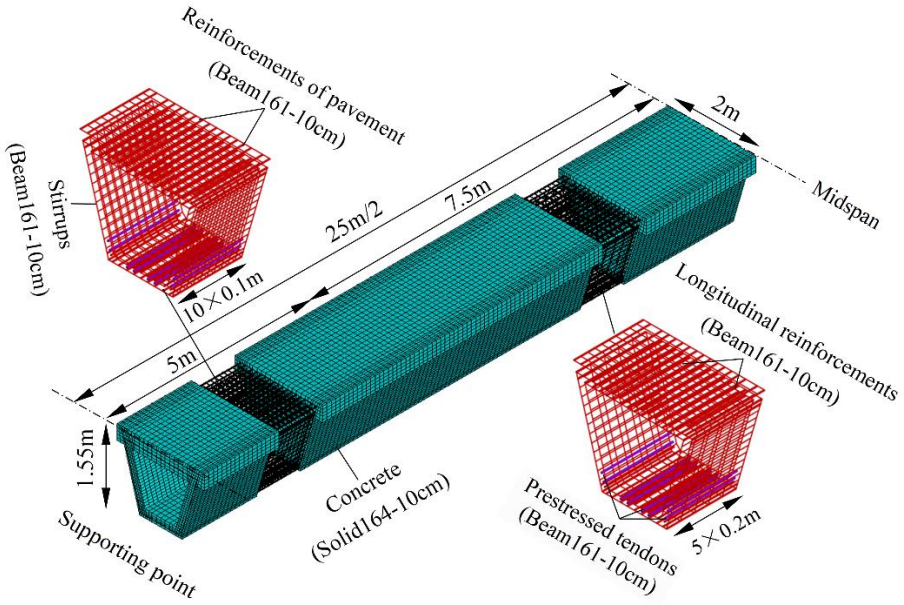

Figure 2. Finite element model of prefabricated small box girder.

High pressure and temperature field were commonly observed during blast wave. Due to the difference in energy transmission and thermal conductivity, the interface between air and structure behaves the characteristic of fluid-solid coupling. The establishment of the air domain and the selection of air pressure are crucial to the accuracy of the calculation results. In order to accurately reflect the blast wave propagation and structural response, the air region is set to 27m×3m×3m to completely wrap the analyzed model as shown in Figure 3.

 doi:10.20944/preprints202403.1125.v1

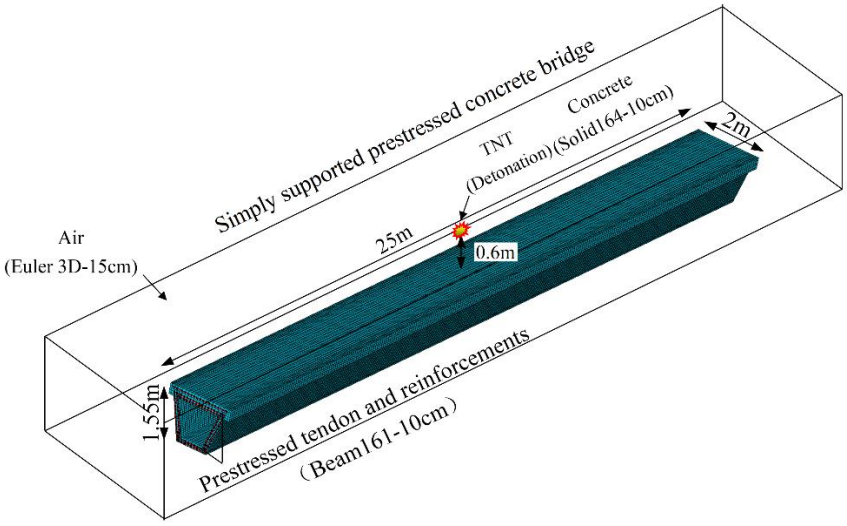

Figure 3. Fluid-solid coupling analysis model under explosion.

In order to obtain the distribution and pressure-time history of the blast wave on the structure, as well as the local response and global damage mode of the beam, gauges are located as shown in Figures 4–6.

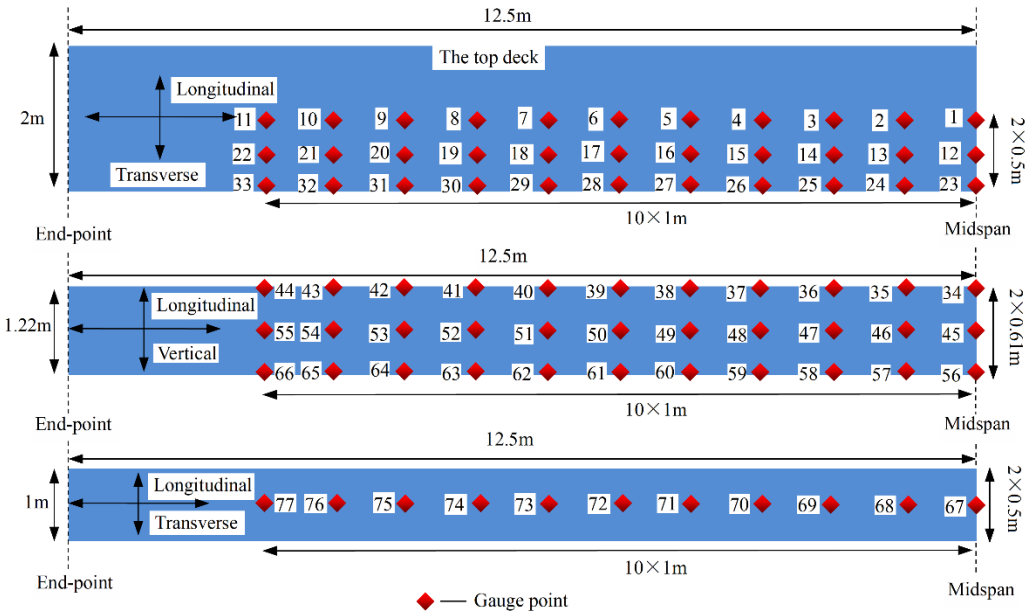

Figure 4. Arrangement of defined gauges in concrete.

Preprints.org (www.preprints.org) | NOT PEER-REVIEWED | Posted: 19 March 2024 doi:10.20944/preprints202403.1125.v1

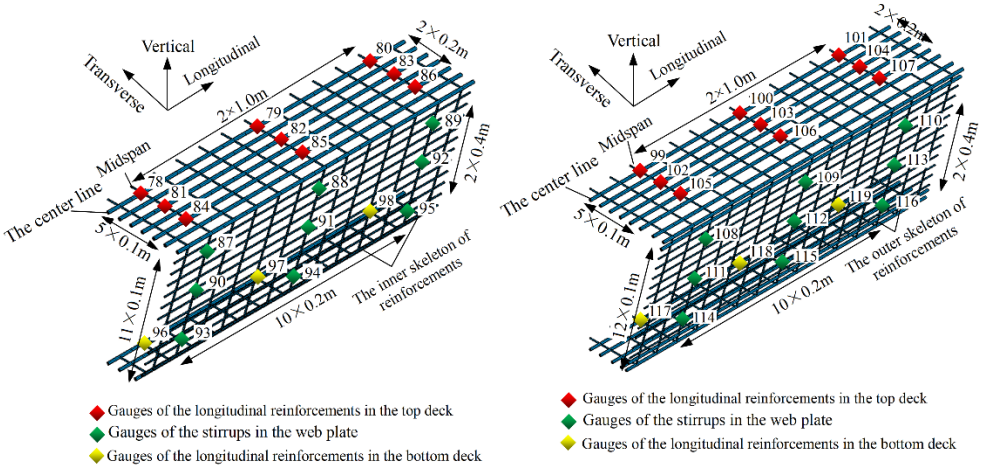

Figure 5. Arrangement of defined gauges in steel bars.

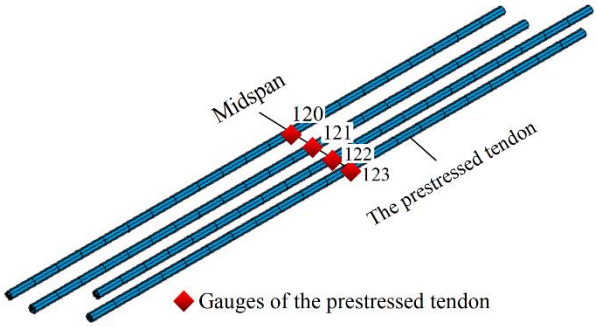

Figure 6. Arrangement of defined gauges in prestressed tendons.

3. Bridge Performance and Result Discussion

3.1. Failure Mode of PSBG

To quantificationally describe the failure mode of PSBG after car explosion, the damage coefficient is presented. With the damage coefficient from 0 to 1, the concrete damage goes from no damage to total failure. Furthermore, the failure mode could be defined by damage coefficient and damage distribution. According to Figure 7, the damage mode of PSBG consists of local flexural failure and global flexural-shear failure under car explosion. The overall flexural-shear failure mode of the structure is basically consistent with Figure 1d, because of the inclined flexural-shear cracks and the distribution of damage zone as shown in Figure 7c. However, due to the framing effect in transverse direction as shown in Figure 8, the tensile zone appears in the lower side of the top deck and the upper side of the bottom deck respectively as shown in Figure 7a,b,d,e. Finally, brittle flexural-shear failure occurs and the bearing capacity is lost.

 doi:10.20944/preprints202403.1125.v1

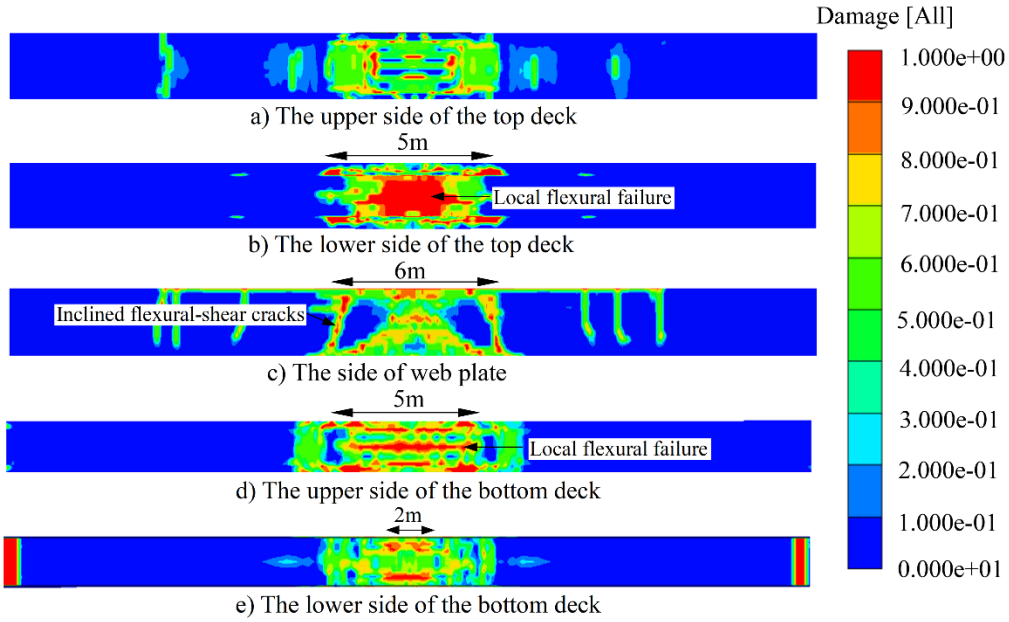

Figure 7. The damage distribution of PSBG under car explosion.

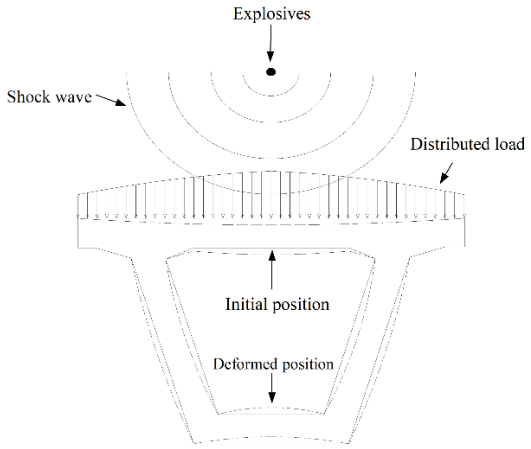

Figure 8. The framing effect of box girder under car explosion.

According to the damage model of the structure under car explosion, preventive strengthening methods are proposed to avoid the sudden collapse of the structure as shown in Figure 9. Strengthening method 1 is expected to prevent the box girder from global flexural-shear failure as depicted in Figure 9b. Except for global flexural-shear failure, local flexural failure in bridge deck should be mitigated or controlled. As a result, strengthening method 2 is presented to enhance the tensile zone of concrete deck as shown in Figure 9c. Further, strengthening method 3 is suggested to concern the transformation of tensile area during reciprocating vibration as indicated in Figure 9d. According to specification for strengthening design [9], the objective of strengthening is to prevent collapse and prompt post-disaster rehabilitation. To balance the construction difficulty and reinforcement effect, the 8mm thick steel plate is adopted. Further, epoxy adhesives and anchor bolts are utilized to avoid slippage and spalling of steel plates. While the adhesive performance and anchor arrangements meet the requirements, node connections can be used between concrete and steel plates.

 doi:10.20944/preprints202403.1125.v1

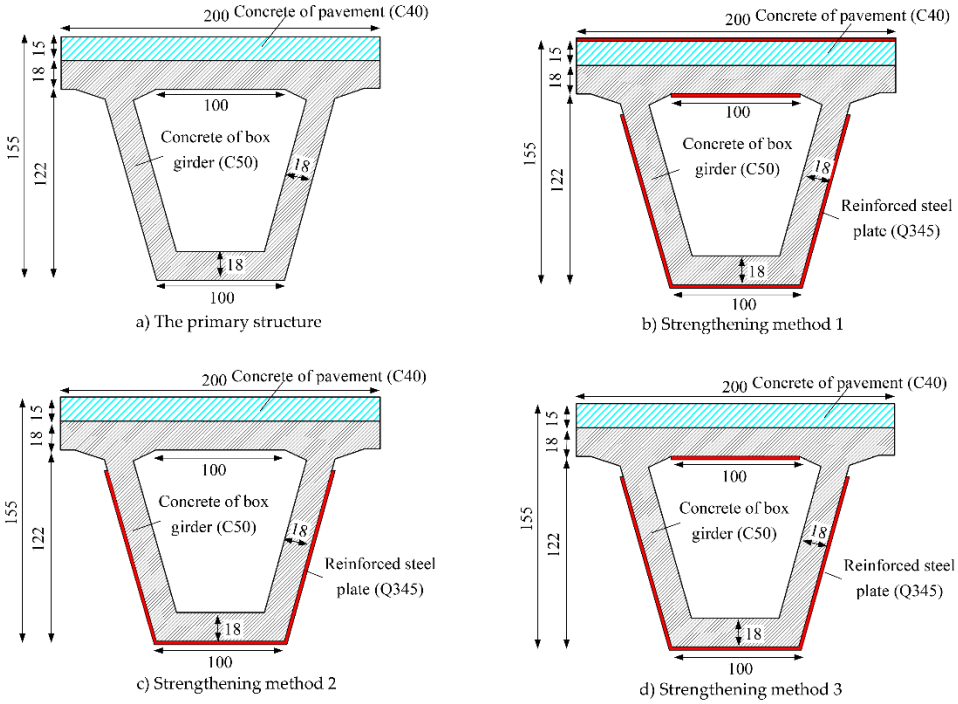

Figure 9. The section of the analytical model (unit: cm).

3.2. Failure Mode of Strengthening Method 1

Sticking the u-shaped steel plate can effectively improve the shear capacity, and the ultimate failure mode of the structure is transformed from flexural-shear failure to flexural failure as shown in Figures 1b and 10c. The U-shaped steel plate improves the shear bearing capacity of the section and reduces the inverted arch of the bottom deck caused by shear deformation. The local failure mode of the bottom deck is controlled by the overall bending failure, which shows that the lower edge of the bottom deck presents more serious failure than the upper edge as shown in Figure 10d,e. The local bending failure of the top deck has not been effectively improved, and the compression area of the section is seriously damaged, which eventually leads to the loss of bending capacity of the structure as shown in Figure 10a–c.

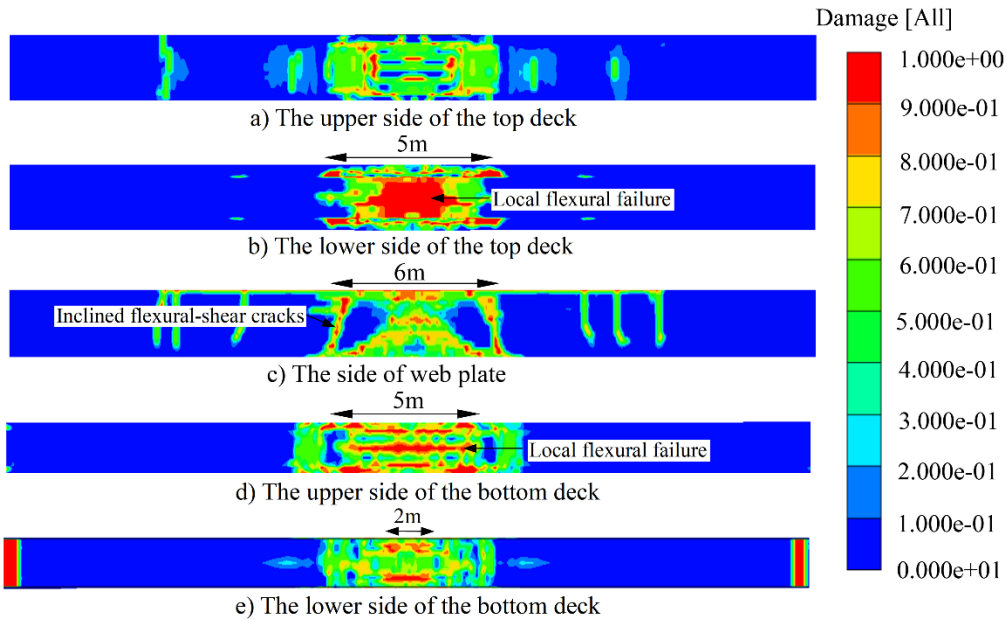

Figure 10. The damage mode of strengthening method 1 after explosion.

 doi:10.20944/preprints202403.1125.v1

3.3. Failure Mode of Strengthening Method 2

In order to enhance the performance of the compressive zone, improve the overall bending resistance of the section, and avoid the bending damage of the structure, the scheme of sticking the steel plate on the lower edge of the top deck is proposed as shown in Figure 9c. Strengthening method 2 can effectively improve the overall bending performance of the structure, and the bending failure height of the structure is reduced to 20 cm as shown in Figure 11c. Figure 11d,e shows that the failure of tensile zone increases corresponding to the failure delay in compression zone, which provide the flexural capacity cooperatively. As the lower edge of the top deck can adapt to greater impact deformation after sticking steel plate, the damaged area of concrete increases, but the overall compressive performance improves as shown in Figure 11a–c.

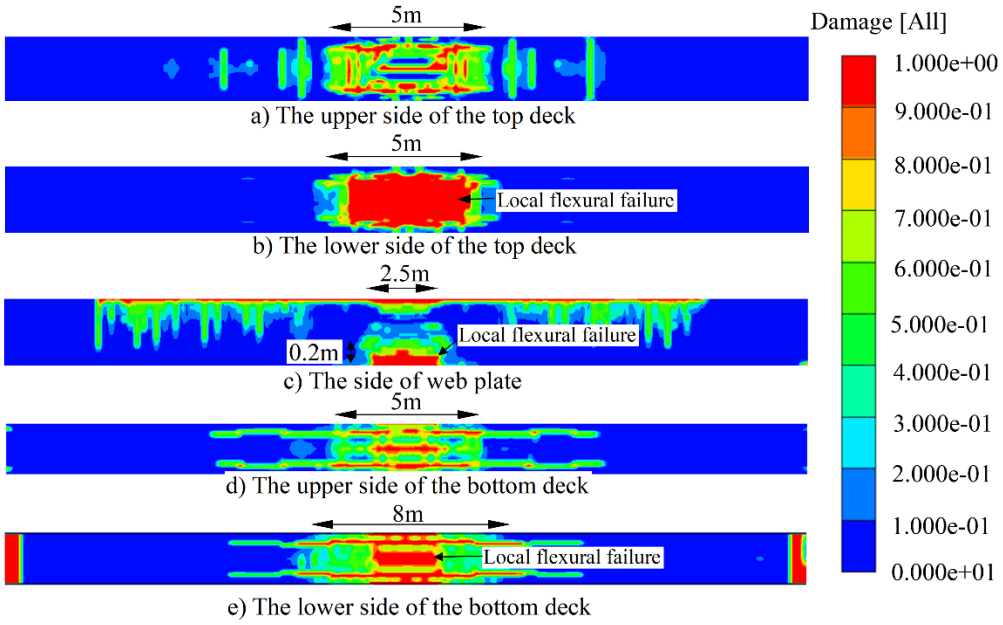

Figure 11. The damage mode of strengthening method 2 after explosion.

3.4. Failure Mode of Strengthening Method 3

Compared with strengthening method 2, strengthening method 3 does not effectively improve the overall flexural performance of the structure and reduce the degree of structural failure under car explosion as shown in Figure 12. As the top surface enhancing with steel plate, the impact energy is concentrated, and the final bending failure height of the structure is increased by 10 cm compared with the reinforced scheme 2. Considering the impact response and strengthening economy of the structure, strengthening method 3 is not recommended.

 doi:10.20944/preprints202403.1125.v1

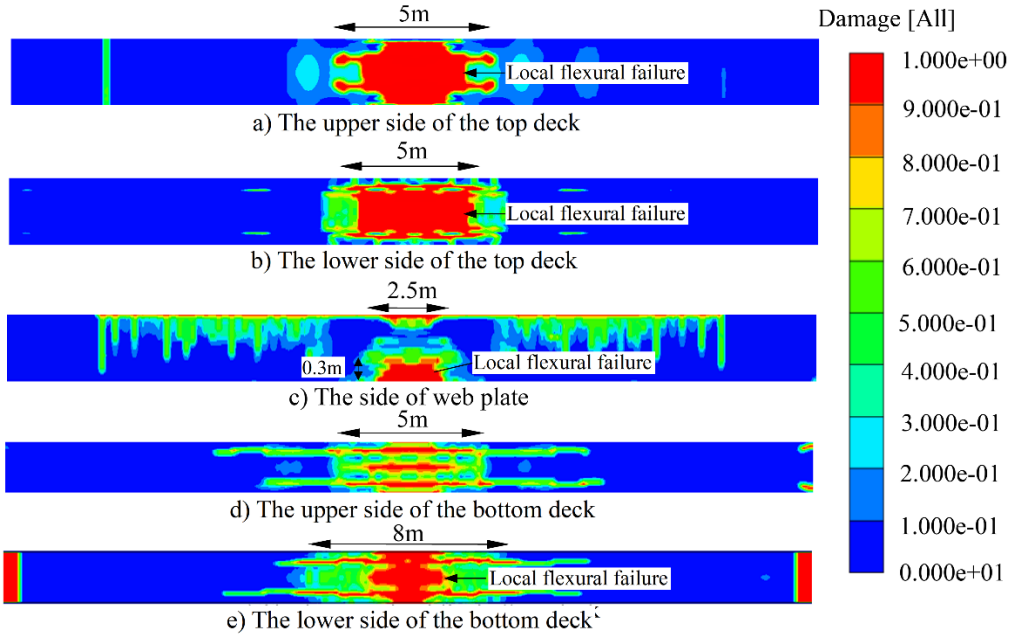

Figure 12. The damage mode of strengthening method 3 after explosion.

4. Discussion of the Failure Mechanism

Due to the instantaneous release of explosive impact energy, the final failure state of the structure was analyzed above. However, during the failure process of the structure, the pressure distribution pattern and the impact failure characteristics of the structure are of great significance. Figure 13 indicates the impact energy dissipates in about 2 ms，except the strengthening method 3 because of energy concentration.

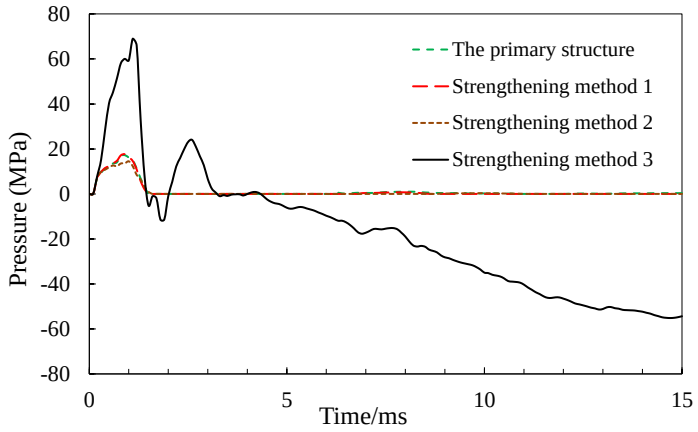

Figure 13. Pressure history of gauge 1.

Sticking U-shaped steel plate can effectively reduce the stress of web concrete and stirrups. The shear strain of concrete is reduced from 2000 to 500, and the shear stress of stirrup is reduced from 200MPa to 118MPa as shown in Figures 14 and 15. The U-shaped steel plate can effectively reduce the tensile stress of the longitudinal steel bar in the lower of the bottom deck, and the reduction range is about 11MPa as shown in Figure 16.

 doi:10.20944/preprints202403.1125.v1

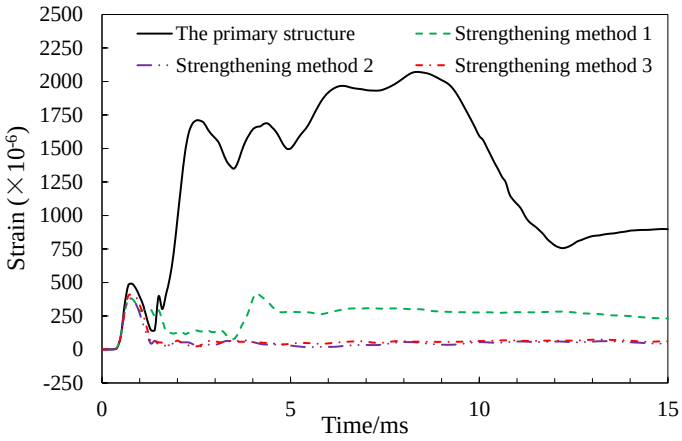

Figure 14. Shear strain-time history of concrete in the web plate (gauge 47).

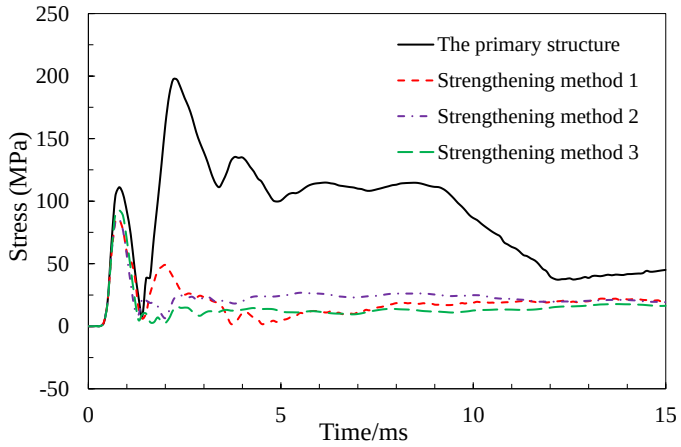

Figure 15. Stress-time history of stirrups in middle of the web plate (gauge 111).

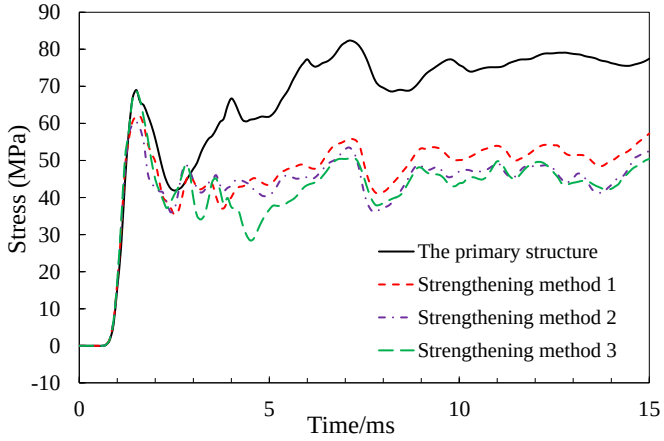

Figure 16. Stress-time history of steel bar in lower of the bottom deck (gauge 117).

Sticking steel plate on the lower edge of the top deck can effectively reduce the compressive strain in the compression and reduce the damage of the concrete under blast loads as shown in Figure 17. Compared with the strengthening method 2, the concrete strain in the compression zone of the strengthening method 3 is larger, as a result of the impact of explosive energy concentration.

 doi:10.20944/preprints202403.1125.v1

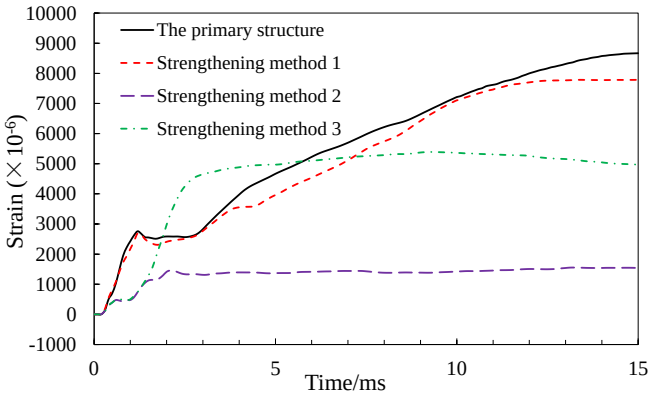

Figure 17. Strain-time history of concrete in the compressive zone (gauge 1).

Figure 18 shows that strengthening structure with bonded steel plate in the lower side of the top deck can improve the tensile stress of steel bars in the top deck, promote a better performance under car explosion. In the process of explosion analysis, the stress increment of prestressed tendon is small, and it will not yield or fracture as shown in Figure 19.

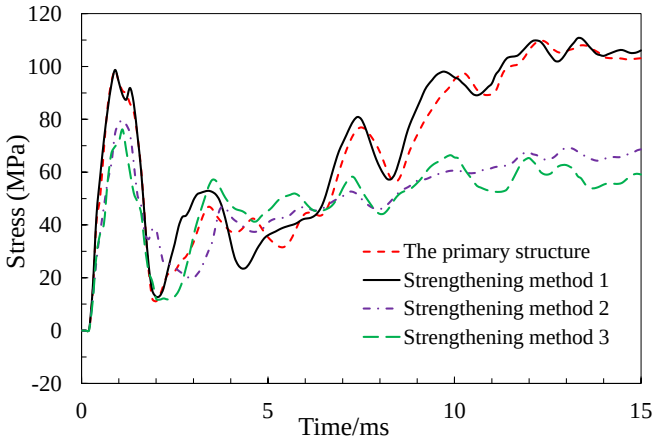

Figure 18. Stress-time history of steel bar in lower of the top deck (gauge 78).

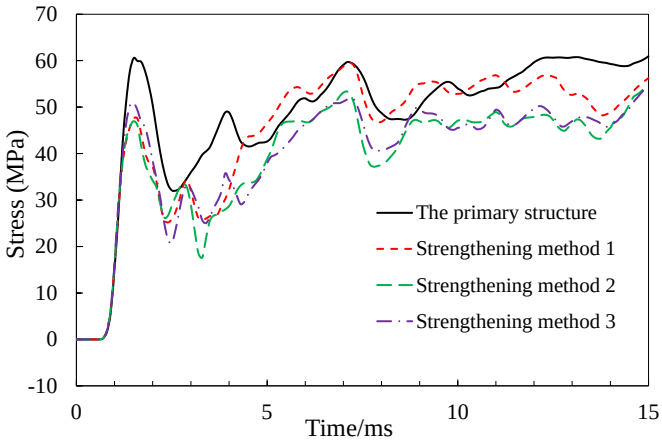

Figure 19. Stress history of prestressed tendon (gauge 120).

5. Conclusions

The purpose of this work is to investigate the failure mechanism and preventive strengthening methods of prefabricated small box girder under car explosion. The structural design of analyzed box girder is in line with the current design specification of RC and PC structures. The 50kg TNT equivalent is placed 0.6 m above bridge deck represent a car explosion in the state of full oil-tank.

After verification by previous studies, three strengthening methods are put forward to improve the performance of precast box girder under car explosion. Further, the antiknock performances of these strengthening methods are discussed. After cautious simulation, the following results can be drawn:

(1) After verification by previous studies, the damage mode of PSBG consists of global flexural-shear failure and local flexural failure under car explosion. To avoid excessive deformation even bridge collapse after car explosion, it is the key to enhance the flexural-shear capacity of the section and the local flexural capacity of the bridge deck. According to the damage mode, U-shape steel plate and flat steel plate are proposed to enhance the global flexural-shear capacity and bending capacity of bridge deck respectively.

(2) Compared with the primary structure, the three strengthening methods can effectively improve the anti-explosion performance of box girder under car explosion. After strengthening with the U-shaped steel plate, the structural failure modes change from global flexural-shear failure to global flexural failure. Adhering steel plate in the lower edge of the top deck can improve the bending capacity of the top deck, reducing the failure in compression zone and strengthening the global flexural resistance. While the steel plate attached to the upper edge of the top deck, the local impact vibration and the bending capacity is strengthened concurrently. As a result, the damage mode is not obviously improved.

(3) Strengthening method 2 is the most effective way to improve the anti-explosion performance of prefabricated small box girder bridges, reducing structural failure, maintaining bearing capacity, avoiding bridge collapse, and buying time for subsequent rescue and maintenance.

Author Contributions: Methodology, WL.H.; software, ZN.Y.; validation, ZN.Y.; formal analysis, ZN.Y.; data curation, FH.D.; supervision, WL.H.; funding acquisition, FH.D. All authors have read and agreed to the published version of the manuscript.

Funding: The Natural Science Foundation of Jiangsu Province (Grant No. BK20200793).

Data Availability Statement: Data is contained within the article.

Conflicts of Interest: The authors declare no conflict of interest.

References

1. Draganić, H.; Gazić, G.; Varevac, D. Experimental Investigation of Design and Retrofit Methods for Blast Load Mitigation – A State-of-the-Art Review. *Engineering Structures* **2019**, *190*, 189–209, doi:10.1016/j.engstruct.2019.03.088.
2. Wang, W.; Liu, R.; Wu, B. Analysis of a Bridge Collapsed by an Accidental Blast Loads. *Engineering Failure Analysis* **2014**, *36*, 353–361, doi:10.1016/j.engfailanal.2013.10.022.
3. Zhai, C.; Chen, L.; Xiang, H.; Fang, Q. Experimental and Numerical Investigation into RC Beams Subjected to Blast after Exposure to Fire. *International Journal of Impact Engineering* **2016**, *97*, 29–45, doi:10.1016/j.ijimpeng.2016.06.004.
4. Zhu, Z.; Li, Y.; He, S.; Ma, C. Analysis of the Failure Mechanism of Multi-Beam Steel–Concrete Composite Bridge under Car Explosion. *Advances in Structural Engineering* **2020**, *23*, 538–548, doi:10.1177/1369433219876185.
5. Hu, Z.; Zhang, Y.; Yu, W.; Mao, S.; Fang, J. Anti-Blast Resistance Analysis of Prestressed Concrete Bridges under Close-by Blast. *China Journal of Highway and Transport* **2019**, *32*, 71–80.
6. Zhang, C.; Gholipour, G.; Mousavi, A.A. Nonlinear Dynamic Behavior of Simply-Supported RC Beams Subjected to Combined Impact-Blast Loading. *Engineering Structures* **2019**, *181*, 124–142, doi:10.1016/j.engstruct.2018.12.014.
7. Shiravand, M.R.; Parvanehro, P. Numerical Study on Damage Mechanism of Post-Tensioned Concrete Box Bridges under Close-in Deck Explosion. *Engineering Failure Analysis* **2017**, *81*, 103–116, doi:10.1016/j.engfailanal.2017.07.033.
8. Lee, J.; Choi, K.; Chung, C. Numerical Analysis-Based Blast Resistance Performance Assessment of Cable-Stayed Bridge Components Subjected to Blast Loads. *Applied Sciences* **2020**, *10*, 8511, doi:10.3390/app10238511.
9. Schmidt, J.W.; Sørensen, J.D.; Christensen, C.O. In Situ Concrete Bridge Strengthening Using Ductile Activated NSMR CFRP System. *Buildings* **2022**, *12*, 2244, doi:10.3390/buildings12122244.

10. Kim, S.-H.; Park, J.-S.; Jung, W.-T.; Kim, T.-K.; Park, H.-B. Experimental Study on Strengthening Effect Analysis of a Deteriorated Bridge Using External Prestressing Method. *Applied Sciences* **2021**, *11*, 2478, doi:10.3390/app11062478.
11. Kim, S.-H.; Park, J.-S.; Jung, W.-T.; Kang, J.-Y. Strengthening Effect of the External Prestressing Method That Simulated a Deterioration Bridge. *Applied Sciences* **2021**, *11*, 2553, doi:10.3390/app11062553.
12. MOT, (Ministry of Transportation) Code for Design of Highway Reinforced Concrete and Prestressed Concrete Bridges and Culverts. *[In Chinese.] JTG D62-2004. Beijing.* **2004**.
13. MOT, (Ministry of Transportation) Specifications for Strengthening Design of Highway Bridges. *[In Chinese.] JTG/T J22-2008. Beijing.* **2008**.
14. Forni, D.; Chiaia, B.; Cadoni, E. Blast Effects on Steel Columns under Fire Conditions. *Journal of Constructional Steel Research* **2017**, *136*, 1–10, doi:10.1016/j.jcsr.2017.04.012.
15. Thomas, R.J.; Steel, K.; Sorensen, A.D. Reliability Analysis of Circular Reinforced Concrete Columns Subject to Sequential Vehicular Impact and Blast Loading. *Engineering Structures* **2018**, *168*, 838–851, doi:10.1016/j.engstruct.2018.04.099.
16. Tu, Z.; Lu, Y. Modifications of RHT Material Model for Improved Numerical Simulation of Dynamic Response of Concrete. *International Journal of Impact Engineering* **2010**, *37*, 1072–1082, doi:10.1016/j.ijimpeng.2010.04.004.
17. Forni, D.; Chiaia, B.; Cadoni, E. Strain Rate Behaviour in Tension of S355 Steel: Base for Progressive Collapse Analysis. *Engineering Structures* **2016**, *119*, 164–173, doi:10.1016/j.engstruct.2016.04.013.
18. Hashemi, S.K.; Bradford, M.A.; Valipour, H.R. Dynamic Response and Performance of Cable-Stayed Bridges under Blast Load: Effects of Pylon Geometry. *Engineering Structures* **2017**, *137*, 50–66, doi:10.1016/j.engstruct.2017.01.032.
19. Williamson, E.B.; Bayrak, O.; Davis, C.; Williams, G.D. Performance of Bridge Columns Subjected to Blast Loads. I: Experimental Program. *J. Bridge Eng.* **2011**, *16*, 693–702, doi:10.1061/(ASCE)BE.1943-5592.0000220.
20. Kyei, C.; Braimah, A. Effects of Transverse Reinforcement Spacing on the Response of Reinforced Concrete Columns Subjected to Blast Loading. *Engineering Structures* **2017**, *142*, 148–164, doi:10.1016/j.engstruct.2017.03.044.
21. Yan, B.; Liu, F.; Song, D.; Jiang, Z. Numerical Study on Damage Mechanism of RC Beams under Close-in Blast Loading. *Engineering Failure Analysis* **2015**, *51*, 9–19, doi:10.1016/j.engfailanal.2015.02.007.
22. Li, J.; Wu, C.; Hao, H.; Su, Y. Experimental and Numerical Study on Steel Wire Mesh Reinforced Concrete Slab under Contact Explosion. *Materials & Design* **2017**, *116*, 77–91, doi:10.1016/j.matdes.2016.11.098.
23. Liu, J.; Yin, Y.; Zhao, Y.; Li, Y. Dynamic Behavior Analysis of I-Shaped RC Beams under Combined Blast and Impact Loads. *Applied Sciences* **2023**, *13*, 1943, doi:10.3390/app13031943.
24. Hao, H.; Tang, E.K.C. Numerical Simulation of a Cable-Stayed Bridge Response to Blast Loads, Part II: Damage Prediction and FRP Strengthening. *Engineering Structures* **2010**, *32*, 3193–3205, doi:10.1016/j.engstruct.2010.06.006.
25. Son, J.; Lee, H.-J. Performance of Cable-Stayed Bridge Pylons Subjected to Blast Loading. *Engineering Structures* **2011**, *33*, 1133–1148, doi:10.1016/j.engstruct.2010.12.031.
26. Tang, E.K.C.; Hao, H. Numerical Simulation of a Cable-Stayed Bridge Response to Blast Loads, Part I: Model Development and Response Calculations. *Engineering Structures* **2010**, *32*, 3180–3192, doi:10.1016/j.engstruct.2010.06.007.
27. Yao, S.; Zhang, D.; Lu, F.; Wang, W.; Chen, X. Damage Features and Dynamic Response of RC Beams under Blast. *Engineering Failure Analysis* **2016**, *62*, 103–111, doi:10.1016/j.engfailanal.2015.12.001.
28. Andreou, M.; Kotsoglou, A.; Pantazopoulou, S. Modelling Blast Effects on a Reinforced Concrete Bridge. *Advances in Civil Engineering* **2016**, *2016*, 1–11, doi:10.1155/2016/4167329.
29. Carta, G.; Stochino, F. Theoretical Models to Predict the Flexural Failure of Reinforced Concrete Beams under Blast Loads. *Engineering Structures* **2013**, *49*, 306–315, doi:10.1016/j.engstruct.2012.11.008.
30. Pan, Y.; Chan, B.Y.B.; Cheung, M.M.S. Blast Loading Effects on an RC Slab-on-Girder Bridge Superstructure Using the Multi-Euler Domain Method. *J. Bridge Eng.* **2013**, *18*, 1152–1163, doi:10.1061/(ASCE)BE.1943-5592.0000457.